DOI 10.4149/BLL_2024_117

Bratisl Med J 2024; 125 (12):
766–774

COMPUTATIONAL STUDY

Computational study of endogenous magnetic particles' effect on action potential processing in a Purkinje cell model

Michal SABO[1], Martin KOPANI[2]

Comenius University, Jessenius Faculty of Medicine, Department of Medical Biophysics, Martin, Slovakia.
martin.kopani@fmed.uniba.sk

ABSTRACT
OBJECTIVES: The study aims to investigate how changes in the conductance of axonal (**Na^+**) and calcium (Ca^{2+}) ion channels affect the generation, course, excitability and firing rate of action potentials in a model of Purkinje cell neurons.
METHODS: The NEURON Simulator was utilized with a Purkinje cell model to investigate generation, time to first spike, firing rate and pattern of action potential (AP) as well as neuronal excitability in relation to the influence of magnetic field on axonal ion channels.
RESULTS: The downregulation of axonal Na^+ and Ca^{2+} conductance led to a significant delay in the generation of the first spike, with completely blocked action potential generation when downregulated by 75%. Conversely, upregulation of axonal Na^+ and Ca^{2+} conductance accelerated the emergence of the first spike.
CONCLUSION: Our findings demonstrate that alterations in ion channel conductance influence the timing and generation of action potentials, suggesting that magnetic fields can modulate neuronal behaviour *(Tab. 4, Fig. 12, Ref. 34)*. Text in PDF www.elis.sk
KEY WORDS: axon, ion channels, conductance, action potential, magnetic field, Purkinje cell.

Introduction

Computational approach in neuroscience has been applied across diverse areas of research. Studies have investigated their application in understanding mental disorders (1, 2, 3) and exploring how animals may utilize magnetoreception in navigation. Evidence from multiple experiments has confirmed the presence of magnetic nanoparticles in human tissues and cells under both physiological and pathological conditions (4, 5, 6). Accumulation of endogenous magnetic particles near Purkinje cell (PC) has been documented by several authors (7, 8, 9). Research has also shown that magnetic fields can affect the shape, size, and integrity of cells in living organisms (10, 11, 12), exerting mechanical, biochemical or physical influences. Iron particles, whether ions, larger molecules or crystals, can mechanically block ion channels (partially or completely) (13, 14). This blockage alters the permeation pathway of ion channels, leading to downregulation of Na^+, K^+ and Ca^{2+} ion channels located on axons and subsequent changes in action potential (AP) processing. Another mechanism through which endogenous magnetic particles influence action potential processing is the production of reactive oxygen species (ROS). Iron, known for inducing ROS species, stimulates ryanodine receptor-mediated calcium release (15). Upregulation of Ca^{2+} ions has a significant impact on Purkinje cell's AP processing. The presence of magnetic nanoparticles on axonal surfaces theoretically affects AP processing due to its influence on ion movement. Numerous experiments have confirmed that weak magnetic fields within the range of up to 10 mT affect AP propagation (16, 17). Purkinje cells are well-studied neuron types located in the cortex of the cerebellum. For computational modelling and simulation purposes, it is necessary to discretise PCs into mathematically describable sections.

Altered conductance of ion channels in PCs can change their response to external and internal stimuli, potentially leading to changes at higher levels of neural function. The response of PCs to magnetic fields is important in the context of neurological diseases with extensive accumulation of magnetic iron in specific parts of the human brain, and neuropsychiatric disorders treated

[1]Comenius University, Jessenius Faculty of Medicine, Department of Medical Biophysics, Martin, Slovakia, and [2]Comenius University, Faculty of Medicine, Institute of Medical Physics and Biophysics, Bratislava, Slovakia

Address for correspondence: Martin KOPANI, RND, Assoc Prof, PhD, Comenius University, Faculty of Medicine, Institute of Medical Physics and Biophysics, Sasinkova 2, SK-813 72 Bratislava, Slovakia.
Phone: +911 9530

Acknowledgements: The authors thank Cedars-Sinai Medical Center's International Research and Innovation in Medicine Program and the Association for Regional Cooperation in the Fields of Health, Technology (RECOOP HST Association) for their support of our study and our organization as a participating Cedars-Sinai Medical Center – RECOOP Research Center (CRRC).

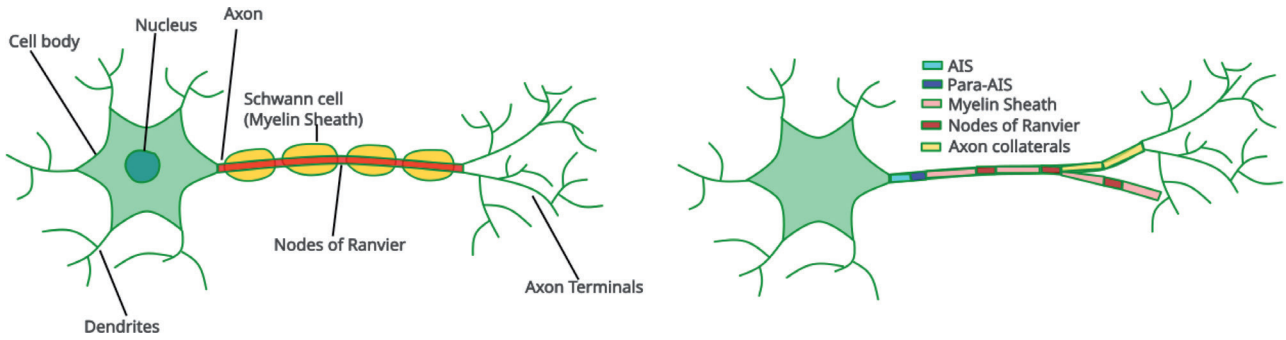

Fig. 1. Left side – Standard composition of a neuron, consisting of a cell body, nucleus, dendrites, axon, Schwann cells (myelin sheaths), nodes of Ranvier, and axon terminals. Right side – Detailed division of axon used in the modelling of the Purkinje cell (11). In this model, the axon is assembled from the axon initial segment (AIS), para-AIS, myelin sheaths, nodes of Ranvier and axon collaterals.

with transcranial magnetic stimulation. The aim of this study is to model the generation and processing of action potential through altering the conductivity of axonal sodium (Na^+) and calcium (Ca^{2+}) ion channels in Purkinje cells, serving as a model for the effect of magnetic fields.

Material and methods

The basic description of the axon includes Schwann cells and nodes of Ranvier. Schwann cells form a myelin sheath that serves as an insulating layer, facilitating faster and more efficient transmission of electrical impulses. Conversely, nodes of Ranvier are not insulated by myelin sheath and are highly enriched by ion channels whose function is to regenerate action potential. In addition, the axon's initial segment, located at the proximal end of the axon, plays a crucial role in initiating the action potential owing to its high concentration of Na+ channels. Furthermore, the concentrations of Na^+, K^+ and Ca^{2+} channels influence not only the spike generation but also spike patterns and spike shapes (18). Additional structures of axon include internodes, paranodes and juxtaparanodes.

We used a detailed model of the Purkinje cell in NEURON (19), with the source code available in ModelDB (20, https://modeldb.science/229585) We selected this model because it is verified, highly detailed (containing 1,611 sections) and has a precise implementation of ionic Na^+, K^+ and Ca^{2+} channels. The computational model was assembled from axonal compartments, including the axon initial segment, paraAIS, four myelinated compartments, three nodes of Ranvier, and two axon collaterals (Fig. 1). Detailed information about the model, along with the rationale behind selecting specific biological, chemical and physical proprieties of the Purkinje cell model, can be found in the original article (21). In our experiments, we modified the channel conductance of the axon compartments. As a benchmark, we used the default values from the model (Tab. 1).

Result

For observing the effect of downregulating Na^+ and Ca^{2+} channels in Purkinje cell axon, we incrementally decreased

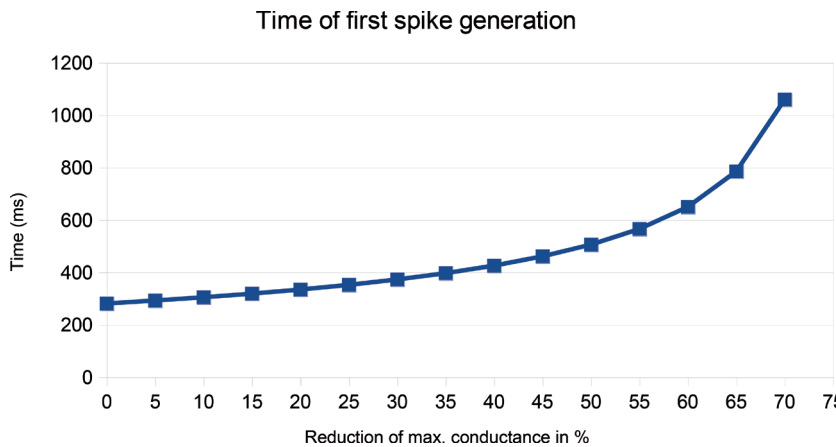

Fig. 2. The change in time up to first spike generation due to reducing maximum conductance of axonal Na^+ and Ca^{2+} channels of Purkinje cell.

Tab. 1. Default values of maximum conductance of axonal Na^+ and Ca^{2+} channels of Purkinje cell.

Channel name	Ion type	Max. conductance	Localization
Cav3.1	**Ca^{2+}**	$8.2 \cdot 10^{-6}$ S/cm^2	Axon initial segment
Nav1.6	**Na^+**	0.50 S/cm^2	Axon initial segment
Cav2.1	**Ca^{2+}**	$2.2 \cdot 10^{-6}$ S/cm^2	Axon initial segment, Ranvier nodes, Axon collateral
Nav1.6	**Na^+**	0.03 S/cm^2	Ranvier nodes, Axon collateral
Cav3.1	**Ca^{2+}**	10^{-5} S/cm^2	Ranvier nodes, Axon collateral

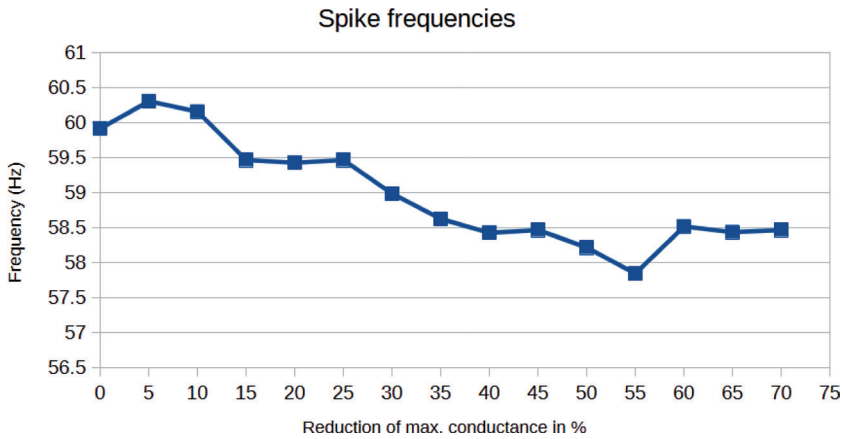

Fig. 3. The change in spike frequencies due to reducing maximum conductance of axonal Na^+ and Ca^{2+} channels of Purkinje cell.

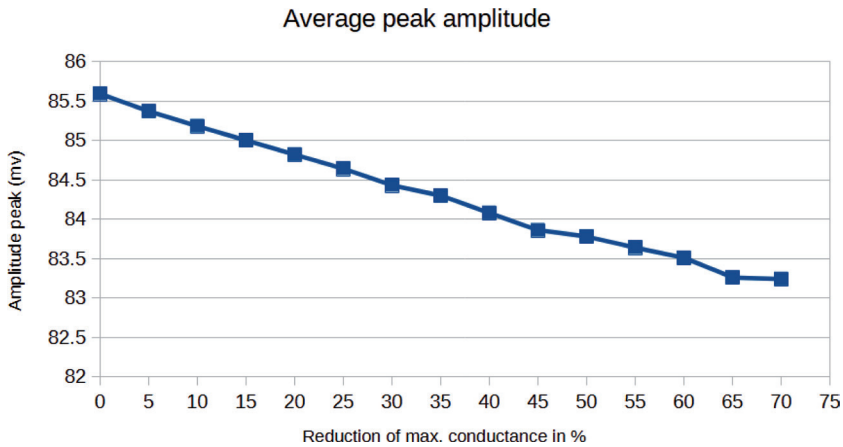

Fig. 4. The change in the amplitude peaks due to reducing maximum conductance of axonal Na^+ and Ca^{2+} channels of Purkinje cell.

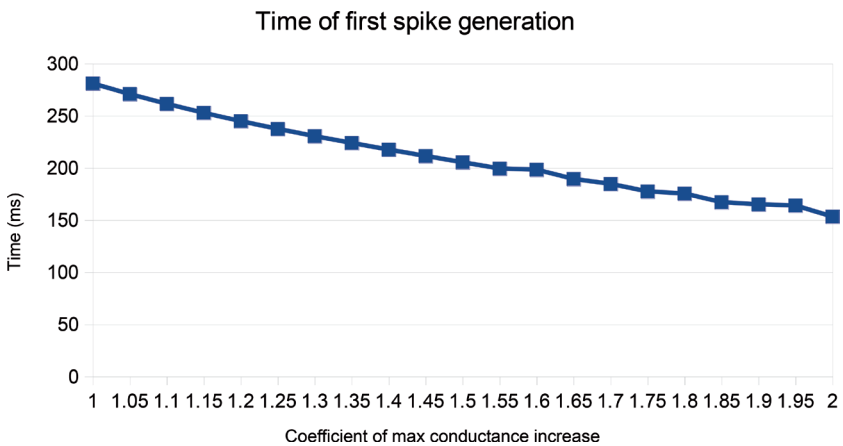

Fig. 5. The change in time up to first spike generation due to increasing maximum conductance of axonal Na^+ and Ca^{2+} channels of Purkinje cell.

their conductance by 5%. Table 2 shows the conductance values of Na^+ and Ca^{2+} channels located on the axon in the Purkinje cell along with the corresponding measured spike frequencies, average peak amplitude, and the time of first spike generation. The most noticeable change was a delay in the generation of the first spike with lower axon Na^+ and Ca^{2+} conductance values (Fig. 2). Spike frequencies oscillated but without signifi ct changes (Fig. 3). Similarly, the peak amplitudes of spikes slightly descended with downregulation, but not significantly (Fig. 4). A downregulation by 75% completely blocked action potential generation.

For observing the effect of upregulating of Na^+ and Ca^{2+} channels in Purkinje cell axon, we increased their conductance in two different sets. First, we incrementally increased their conductance by 5% of their original values (increase coefficient of 0.05). Table 3 shows the conductance values, measured spike frequencies, average peak amplitude and time of first spike generation. Second, we incrementally increased their conductance by 100% of their original values (increase coefficient of 1). Table 4 shows the corresponding conductance values, measured spike frequencies, average peak amplitude, and time of first spike generation. In both upregulation sets, the cell generated the first spike earlier with higher axon Na^+ and Ca^{2+} conductance (Figs 5 and 6).

Spike frequencies (Fig. 7) decreased at the beginning of the first testing set, but then increased and continued to rise in the second testing test (Fig. 8). Notably, it was observed that with coefficient 1.40, the spike frequency intensified. In the AP graph (Fig. 9), there is a visible dent in spike generation, marking an emergent spike notch. This notch, an irregularity or abnormal course of AP initially appeared with every second spike. With higher conductance (up to coefficient of 2), the emergence of notches gained in frequency. For coefficients 3, 4 and 6, no spike notches were observed. For coefficients 5, 7, 8 and 9, the pattern of spike notch occurrence became irregular, and the generation of spikes came to a complete halt after a while with coefficient 9 (Fig. 10.).

In the first testing set (increase coefficient of 0.05), the peak amplitude of spikes increased with upregulation (Fig. 11). However, in the second testing set (increase coefficient of 1), the peak amplitude initially increased before decreasing (Fig. 12).

Discussion

Magnetic fields induced by particles have the potential to affect biological and chemical processes, including ion distribution. Understanding how the endogenous magnetic fields on axon surfaces affect the primary axonal function, i.e., AP processing, is crucial. In Purkinje cell, AP propagation in axons involves the movement of Na^+, K^+ and Ca^{2+} ions (22, 23) along and perpendicular to the axon axis. Magnetic fields exert Lorentz force on ions, acting either attractively or a repulsively, depending on the magnetic particle's orientation. These forces alter ion distributions, poten-

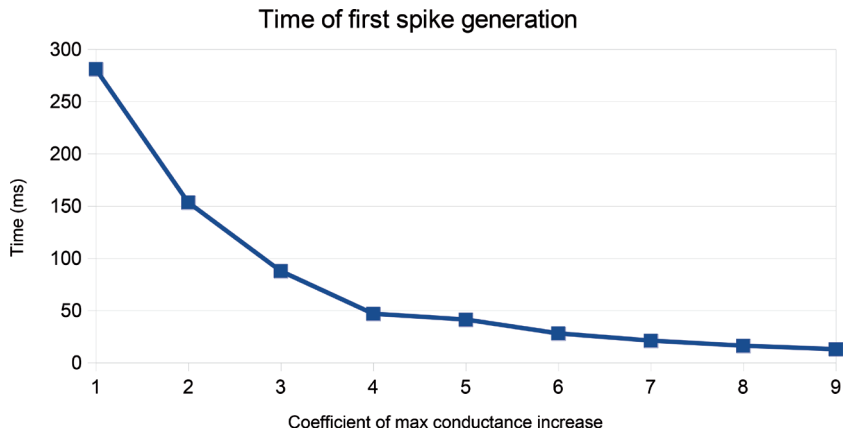

Fig. 6. The change in time up to first spike generation due to increasing maximum conductance of axonal Na^+ and Ca^{2+} channels of Purkinje cell.

Tab. 2. Conductance of Na^+ and Ca^{2+} channels on axon in Purkinje cell and the measured spike frequencies, average amplitude peak and the time of generation of the first spike during downregulation.

Reduction (%)	Na1.6 in Axon initial segment	Ca2.1 in Axon initial segment	Ca3.1 in Axon initial segment	Na1.6 in Ranvier nodes and Axon collateral	Ca2.1 in Ranvier nodes and Axon Collateral	Ca3.1 in Ranvier nodes and Axon collateral
1	0.5	0.00022	0.000008	0.03	0.00022	0.00001
0.95	0.475	0.000209	0.00000779	0.0285	0.000209	0.0000095
0.9	0.45	0.000198	0.00000738	0.027	0.000198	0.000009
0.85	0.425	0.000187	0.00000697	0.0255	0.000187	0.0000085
0.8	0.4	0.000176	0.00000656	0.024	0.000176	0.000008
0.75	0.375	0.000165	0.00000615	0.0225	0.000165	0.0000075
0.7	0.35	0.000154	0.00000574	0.021	0.000154	0.000007
0.65	0.325	0.000143	0.00000533	0.0195	0.000143	0.0000065
0.6	0.3	0.000132	0.00000492	0.018	0.000132	0.000006
0.55	0.275	0.000121	0.00000451	0.0165	0.000121	0.0000055
0.5	0.25	0.00011	0.0000041	0.015	0.00011	0.000005
0.45	0.225	0.000099	0.00000369	0.0135	0.000099	0.0000045
0.4	0.2	0.000088	0.00000328	0.012	0.000088	0.000004
0.35	0.175	0.000077	0.00000287	0.0105	0.000077	0.0000035
0.3	0.15	0.000066	0.00000246	0.009	0.000066	0.000003
0.25	0.125	0.000055	0.00000205	0.0075	0.000055	0.0000025

Reduction (%)	First spike at (ms)	Frequency (Hz)	Average amplitude (mV)
1	280.975	59.92	85.59
0.95	292.2	60.31	85.37
0.9	304.65	60.16	85.18
0.85	318.525	59.47	85
0.8	334.175	59.43	84.82
0.75	352	59.47	84.64
0.7	372.525	58.99	84.43
0.65	396.675	58.63	84.3
0.6	425.5	58.43	84.08
0.55	460.875	58.47	83.86
0.5	505.75	58.22	83.78
0.45	565.325	57.85	83.64
0.4	650	58.52	83.51
0.35	785.175	58.44	83.26
0.3	1059.35	58.47	83.24
0.25	NA	NA	NA

tially upregulating or downregulating ion channel conductance. Due to their charge, Ca^{2+} ions are subjected to greater force than Na^{+} and K^{+} ions at the same ion velocities. The magnetic field also curves ion trajectories, which depends directly on ion mass, and velocity, and inversely on ion charge, and magnetic flux density (magnetic field strength). Consequently, various ions moving perpendicular to the axis of axon through channels located in specific regions such as the axon initial segment (AIS), nodes of Ranvier (NR) or collateral segment, follow trajectories with distinct curvatures. Ions with the lowest mass (Na^{+}) and those with the highest charge (Ca^{2+}) exhibit the greatest curvatures in their trajectories. These trajectory curvatures within regions of conduction may increase friction between ions and channel walls (24), influencing the upregulation and downregulation of sodium

Tab. 3. Conductance of Na^{+} and Ca^{2+} channels on axon in Purkinje cell and the measured spike frequencies, average amplitude peak and the time of generation of the first spike during upregulation by coefficient 0.05.

Coefficient	Na1.6 in Axon initial segment	Ca2.1 in Axon initial segment	Ca3.1 in Axon initial segment	Na1.6 in Ranvier nodes and Axon collateral	Ca2.1 in Ranvier nodes and Axon Collateral	Ca3.1 in Ranvier nodes and Axon collateral
1	0.5	0.00022	0.000008	0.03	0.00022	0.00001
1.05	0.525	0.000231	0.00000861	0.0315	0.000231	0.0000105
1.1	0.55	0.000242	0.00000902	0.033	0.000242	0.000011
1.15	0.575	0.000253	0.00000943	0.0345	0.000253	0.0000115
1.2	0.6	0.000264	0.00000984	0.036	0.000264	0.000012
1.25	0.625	0.000275	0.00001025	0.0375	0.000275	0.0000125
1.3	0.65	0.000286	0.00001066	0.039	0.000286	0.000013
1.35	0.675	0.000297	0.00001107	0.02	0.000297	0.0000135
1.4	0.7	0.000308	0.00001148	0.042	0.000308	0.000014
1.45	0.725	0.000319	0.00001189	0.0435	0.000319	0.0000145
1.5	0.75	0.00033	0.0000123	0.045	0.00033	0.000015
1.55	0.775	0.000341	0.00001271	0.0465	0.000341	0.0000155
1.6	0.8	0.000352	0.00001312	0.048	0.000352	0.000016
1.65	0.825	0.000363	0.00001353	0.0495	0.000363	0.0000165
1.7	0.85	0.000374	0.00001394	0.051	0.000374	0.000017
1.75	0.875	0.000385	0.00001435	0.0525	0.000385	0.0000175
1.8	0.9	0.000396	0.00001476	0.054	0.000396	0.000018
1.85	0.925	0.000407	0.00001517	0.0555	0.000407	0.0000185
1.9	0.95	0.000418	0.00001558	0.057	0.000418	0.000019
1.95	0.975	0.000429	0.00001599	0.0585	0.000429	0.0000195
2	1	0.00044	0.0000164	0.06	0.00044	0.00002

Coefficient	First spike at (ms)	Frequency (Hz)	Average amplitude (mV)
1	280.975	59.92	85.59
1.05	270.75	60.14	85.74
1.1	261.425	60.39	85.98
1.15	252.8	60.1	86.18
1.2	244.825	60.39	86.41
1.25	237.4	60.14	86.64
1.3	230.45	59.9	86.96
1.35	223.9	56.3	87.75
1.4	217.55	57.79	87.82
1.45	211.4	54.79	88.44
1.5	205.4	54.61	88.84
1.55	199.375	53.87	89.23
1.6	198.3	53.28	89.64
1.65	189.4	52.47	90.15
1.7	184.675	51.78	90.48
1.75	177.425	51.03	91.07
1.8	175.45	50.97	91.42
1.85	167.075	50.74	91.98
1.9	164.975	51.23	92.32
1.95	163.925	52.29	92.7
2	153.275	53.07	92.98

Na^+ and Ca^{2+} ion channels in response to magnetic fields.

The axon initial segment (AIS) is characterized by a high density of voltage-gated Na^+, K^+ and Ca^{2+} channels (25). Na^+ channels are effective spike generators in the AIS, facilitating rapid depolarization during the action potential during sodium ions' influx into the cell. Their inactivation can lead to AP firing blockage or reduced firing frequency (26). Blocking Na^+ channels has been shown to increase spontaneous AP generation (27) and reduce spike amplitude. Ca^{2+} channels are primarily involved in neurotransmitter release and synaptic plasticity. They can also influence AP initiation. Their blockage, mediated by neuromodulators activity can influence neuronal firing patterns (18, 28) albeit with marginal effect on spike generation. Reducing the conductance of both sodium and calcium channels may result in decreased AP amplitude, altered firing pattern, reduced firing frequency, and prolonged time to first spike (TFS) emergence, which represents time required to generate the first AP in response to a stimulus. TFS can be influenced by factors such as resting membrane potential, membrane excitability, ion channel conductance, and neuromodulatory activity. Our findings show that TFS increases from approximately 281 ms to 1,059 ms with increasing reduction in Na^+ and Ca^{2+} channel conductance. We also observed a slight decrease in frequency from approximately 60 Hz to 58.5 Hz, while the amplitude of AP remained almost constant. Some of our results are consistent with those of other authors.

Sodium voltage-gated channels open during the depolarization phase of AP, allowing an influx of Na^+ ions into the cell in response to a stimulus. Upregulation of Na^+ channels may enhance the excitability of Purkinje cells, leading to a reduction in TFS as a result of increased Na^+ ion influx. Ca^{2+} channels, while not directly involved in AP generation, play a crucial role. They can activate calcium-dependent processes in the neuron through various intracellular signalling pathways and modulate the activity of voltage-gated ion channels (including sodium channels). Increased Ca^{2+} influx influences the activation rate of calcium-dependent processes (29). In our model, upregulation of Na^+ and Ca^{2+}channels resulted in a linear decrease in TFS from approximately 281 ms to 153 ms across a range of conductance up to twice the initial value. Subsequently, TSF decreased exponentially until it disappeared. Yucel et al. (30) investigated the effect of 2.45 GHz

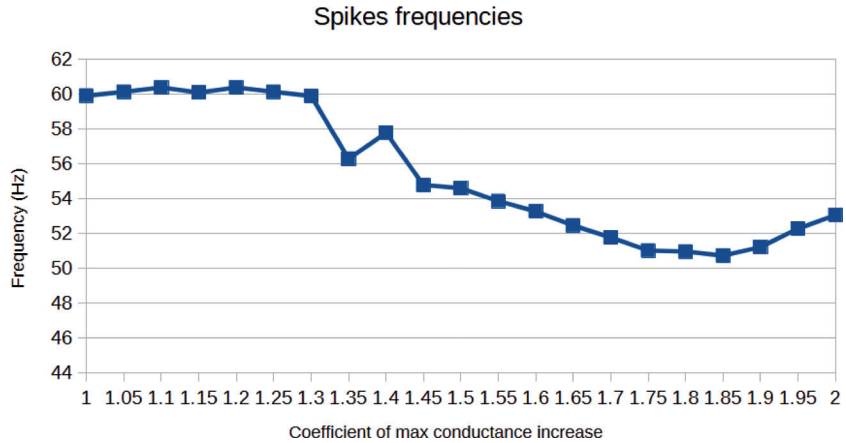

Fig. 7. The change in spike frequencies due to increasing maximum conductance of axonal Na^+ and Ca^{2+} channels off Purkinje cell.

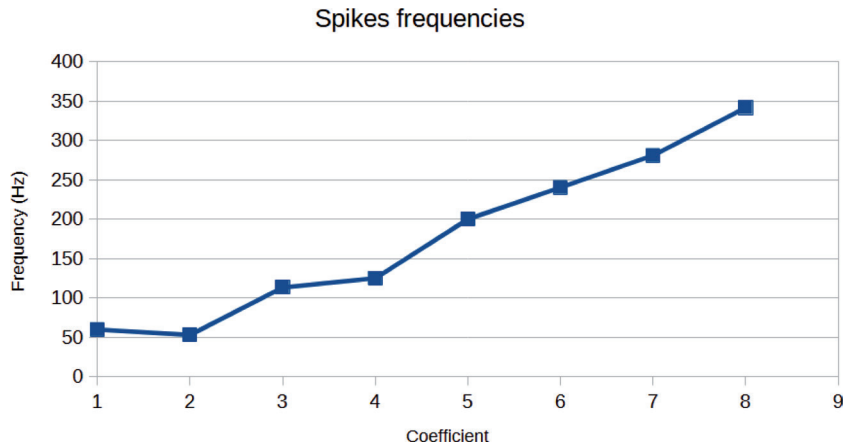

Fig. 8. The change in spike frequencies due to increasing maximum conductance of axonal Na^+ and Ca^{2+} channels of Purkinje cell.

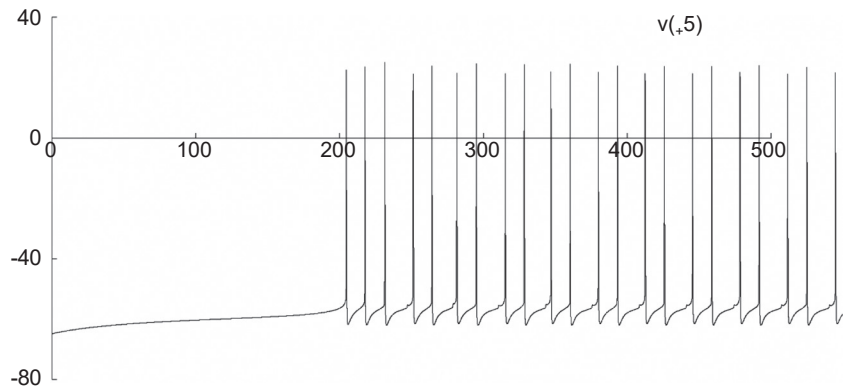

Fig. 9. The emergence of spike notch following the increase in conductance by coefficient of 1.40.

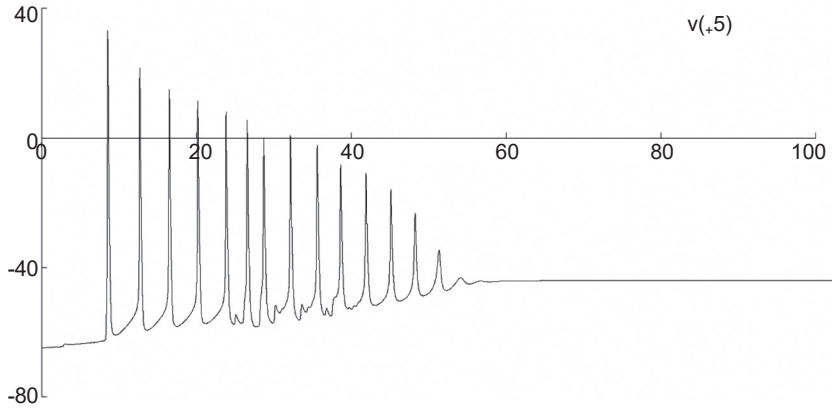

Fig. 10. Increasing conductance by coefficient of 9 halted spike generation.

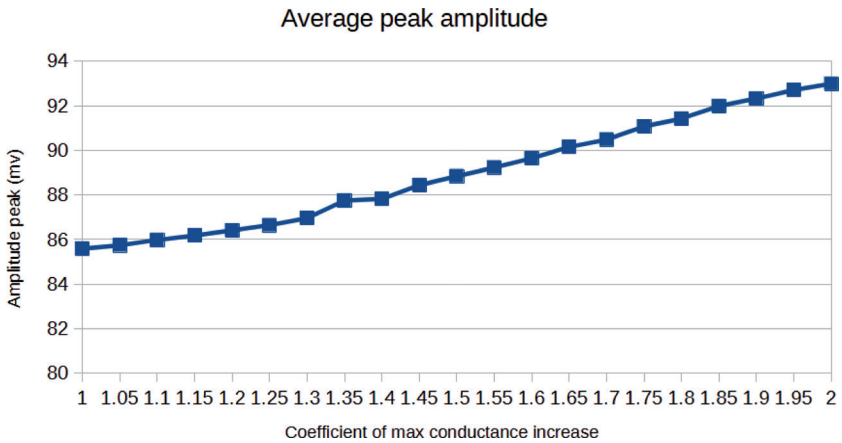

Fig. 11. The change in peak amplitudes due to increasing maximum conductance of axonal Na^+ and Ca^{2+} Purkinje cell channels.

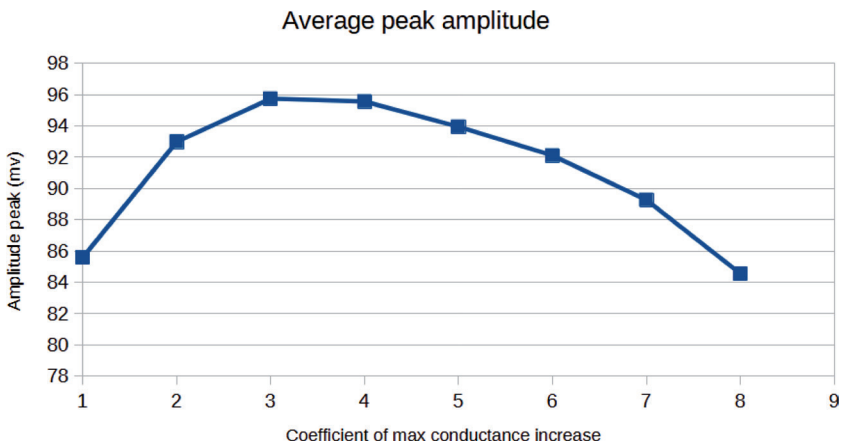

Fig. 12. The change in the peak amplitudes due to increasing maximum conductance of axonal Na^+ and Ca^{2+} channels of Purkinje cell.

electromagnetic field on rats and found a significant reduction in TFS in exposed animals. In addition, the upregulation of neurons can lead to higher firing frequences, indicating an increased rate of AP spikes generation. Our results initially showed a decrease in the frequency rate of AP spikes generation, followed by its increase. Similarly, Kispersky et al. (31) observed reduced firing rates with increased sodium conductance.

Altered conductance through upregulation or downregulation of ion channels can result from the Lorentz force and curved trajectory of ions in a magnetic field. Since Na^+ and Ca^{2+} are more affected than K^+ ions, we adjusted the conductance of these ion channels in our model. We did not account for other factors such as the induction of electric fields in axons, which can significantly influence voltage-gated ion channels, molecular arrangement of membrane, and other effects (32). Some studies have observed through computational modelling that moderate static magnetic fields cannot markedly influence the propagation of action potential along the axis of axon (33, 34). Theoretical calculation revealed that a magnetic field with a flux density of 25 T could reduce AP propagation by 10% due to the deflection of ion flow in the axon. These results support the established notion that magnetic fields significantly influence membrane ion channels.

Conclusion

Computational neuroscience aids understanding how the brain processes information and generates action potential through various factors using computational models and simulations. In this study, we used the model of Purkinje cells to simulate the impact of magnetic fields on action potential generation and processing in axon. Our results indicate that magnetic fields can significantly affect the functioning of Purkinje cells. Specifically, the Lorentz force and curvature of ions trajectory caused by the magnetic field lead to upregulation and downregulation of Na^+ and Ca^{2+} ion channels. These changes result in altered TFS, frequency of AP spike generation, and AP amplitude. Studying the impact of magnetic fields on neurons could elucidate the effects of magnetic iron accumulation in various neurological diseases and inform the application of transcranial magnetic stimulation.

Tab. 4. Conductances of Na^+ and Ca^{2+} channels on axon in Purkinje cell and the measured spike frequencies, average amplitude peak and the time of generation of the first spike during upregulation by coefficient 1.

Coefficient	Na1.6 in Axon initial segment	Ca2.1 in Axon initial segment	Ca3.1 in Axon initial segment	Na1.6 in Ranvier nodes and Axon collateral	Ca2.1 in Ranvier nodes and Axon Collateral	Ca3.1 in Ranvier nodes and Axon collateral
1	0.5	0.00022	0.000008	0.03	0.00022	0.00001
2	1	0.00044	0.0000164	0.06	0.00044	0.00002
3	1.5	0.00066	0.0000246	0.09	0.00066	0.00003
4	2	0.00088	0.0000328	0.12	0.00088	0.00004
5	2.5	0.0011	0.000041	0.15	0.0011	0.00005
6	3	0.00132	0.0000492	0.18	0.00132	0.00006
7	3.5	0.00154	0.0000574	0.21	0.00154	0.00007
8	4	0.00176	0.0000656	0.24	0.00176	0.00008
9	4.5	0.00198	0.0000738	0.27	0.00198	0.00009

Coefficient	First spike at (ms)	Frequency (Hz)	Average amplitude (mV)
1	280.975	59.92	85.59
2	153.275	53.07	92.98
3	87.475	113.46	95.74
4	46.65	124.91	95.56
5	41.075	200.11	93.95
6	27.825	240.34	92.11
7	20.9	280.94	89.27
8	16	341.73	84.56
9	12.65	NA	NA

References

1. Mäki-Marttunen T, Kaufmann T, Elvsåshagen T, Devor A, Djurovic S, Westlye LT, Andreassen OA. Biophysical psychiatry – How computational neuroscience can help to understand the complex mechanisms of mental disorders. Frontiers Psych 2019; 10: 534.

2. Nichols S, Havens L, Taylor B. Sensation to navigation: A Computational neuroscience approach to magnetic field navigation. J Compar Physiol A 2022; 208 (1): 167–176.

3. Taylor BK, Johnsen S, Lohmann KJ. Detection of magnetic field properties using distributed sensing: A computational neuroscience approach. Bioinspir Biomimet 2017; 12 (3): 036013.

4. Maher BA, Ahmed IA, Karloukovski V et al. Magnetite pollution nanoparticles in the human brain PNAS 2016; 113: 10797–10801.

5. Giere R. Magnetite in the human body: Biogenic vs. anthropogenic. PNAS 2016; 113: 11986–11987.

6. Alkhateeb AA, Connor JR. The significance of ferritin in cancer: antioxidation, inflammation and tumorigenesis. Biochim. Biophys. Acta – Rev. Cancer 2013; 1836: 245–254.

7. Levi S, Finazzi D. Neurodegeneration with brain iron accumulation: update on pathogenicmechanisms. Frontiers Pharm 2014; 5: 88017.

8. Gulturk S, Kozan R, Bostanci M, Sefil F, Bagirici F. Inhibition of neuronal nitric oxide synthase prevents iron-induced cerebellar Purkinje cell loss in therat. Acta neurobiol experimentalis 2008; 68 (1): 26–31.

9. Misek J, Veterník M, Tonhajzerova I et al. Radiofrequency electromagnetic field affects heart rate variability in rabbits. Physiol Res 2020; Aug 31; 69 (4): 633–643.

10. Hernando A, Galvez F, García MA et al. Effects of moderate static magnetic field on neural systems Is a non-invasive mechanical stimulation of the brain possible theoretically? Front. Neurosci 2020; 14: 495451.

11. Teodori L, Albertini MC, Uguccioni F et al. Static magnetic fields affect cell size, shape, orientation, and membrane surface of human glioblastoma cells, as demonstrated by electron, optic, and atomic forcemicroscopy. Cytometry Part A: J. Int. Soc. Anal. Cytology 2006; 69: 75–85.

12. Zablotskii V, Polyakova T, Lunov O, Dejneka A. How a high-gradient magnetic field could affect cell life Sci. Rep 2016; 6: 1–13.

13. Nakamichi N, Ohno H, Nakamura Y, Hirai T, Kuramoto N, Yoneda Y. Blockade by ferrous iron of Ca2+ influx through N-methyl-D-aspartate receptor channels in immature cultured rat cortical neurons. J Neurochem 2002; 83 (1): 1–11.

14. Rampersaud S, Fang J, Wei Z, Fabijanic K, Silver S, Jaikaran T, Matsui H. The effect of cage shape on nanoparticle-based drug carriers: anticancer drug release and efficacy via receptor blockade using dextran-coated iron oxide nanocages. Nano let 2016; 16 (12): 7357–7363.

15. Hidalgo C, Núñez MT. Calcium, iron and neuronalfunction. IUBMB life 2007; 59 (4–5): 280–285.

16. Hong C, Huestis P, Thompson R, Yu J. Learning ability of young rats is unaffected by repeated exposure to a static electromagnetic field in early life. Bioelectromag 1988; 9: 269–273

17. Rosen MS, Rosen AD. Magnetic field influence on Parameciummotility. Life Sci 1990; 46: 1509–1515

18. Bender KJ, Trussell LO. The physiology of the axon initial segment. Ann Rev Neurosci 2012; 35: 249–65.

19. Hines ML, Carnevale NT. Neuron: A tool for neuroscientists. The Neuroscientist 2001; 7: 123–135.

20. McDougal RA, Morse TM, Carnevale T et al. Twenty years of ModelDB and beyond: building essential modeling tools for the future of neuroscience. J.Comput.Neurosci 2017; 42: 1.

21. Masoli S, Solinas S, D'Angelo E. Action potential processing in a detailed Purkinje cell model reveals a critical role for axonal compartmentalization. Front. Cell. Neurosci 2015; 9: 47–68.

22. Callewaert G, Eilers J, Konnerth A. Axonal calcium entry during fast 'sodium' action potentials in rat cerebellar Purkinje neurones. J Physiol 1996; 495 (Pt 3): 641–647.

23. Monsivais P, Clark BA, Roth A, Häusser M. Determinants of action potential propagation in cerebellar Purkinje cell axons. J Neurosci 2005; 25 (2): 464–472.

24. Freire MJ, Bernal-Méndez J, Pérez AT. The Lorentz force on ions in membrane channels of neurons as a mechanism for transcranial static magnetic stimulation. Electromag Biol Med 2020; 39 (4): 310–315.

25. Colbert C, Pan E. Ion channel properties underlying axonal action potential initiation in pyramidal neurons. Nat Neurosci 2002; 5: 533–538.

26. Schonewille M, Sara K, Winkelman BHJ, Hoebeek FE, Jeu MTGD, Larsen IM et al. Purkinje cells in awake behaving animals operate at the upstate membrane potential. Nat. Neurosci 2006; 9, 459–461.

27. Schmid G, Goychuk I, Hänggi, P. Effect of channel block on the spiking activity of excitable membranes in a stochastic Hodgkin–Huxley model. Phys Biol 2004; 1 (2): 61.

28. Bender KJ, Ford CP, Trussell LO. Dopaminergic modulation of axon initial segment calcium channels regulates action potential initiation. Neuron 2010; 68 (3): 500–511.

29. Bender KJ, Trussell LO. Axon initial segment Ca^{2+} channels influence action potential generation and timing. Neuron 2009; 61 (2): 259–271.

30. Yucel H, Dundar NO, Doguc DK, Uguz C, Celik O, Aksoy FT, Dundar B. Evaluation of cognitive functions and EEG records in rats exposed to 2.45 GHz electromagnetic field. International J Rad Res 2022; 20 (4): 753–760.

31. Kispersky TJ, Caplan JS, Marder E. Increase in sodium conductance decreases firing rate and gain in model neurons. J Neurosci 2012; 32 (32): 10995–11004.

32. Hashemi S, Abdolali A. Three-dimensional analysis, modeling, and simulation of the effect of static magnetic fields on neurons. Bioelectromag 2017; 38 (2): 128–136.

33. Jamasb S. Extension of the neuronal membrane model to account for suppression of the action potential by a constant magnetic field. Biophys 2017; 62: 428–433.

34. Wikswo JP, Barach JP, Freeman JA. Magnetic field of a nerve impulse: first measurements. Science 1980; 208 (4439): 53–55.

Received May 5, 2024.
Accepted July 17, 2024.